Polarization Insensibility of Columnar Quantum Dot Structure Emitting at $\lambda = 1.55$ μm: A Theoretical Study

Jacky Even, Laurent Pedesseau

Polarization Insensibility of columnar quantum dot structure emitting at λ=1.55μm : a theoretical study

J. Even[a)] **and L. Pedesseau.**

FOTON-INSA Laboratory, UMR 6082 au CNRS, INSA de Rennes, 20 Avenue des Buttes de Coësmes, CS 14315, 35043 Rennes Cedex, France

Abstract.

Vertically stacked InAs/InP columnar quantum dots (CQD) for polarization insensitive semiconductor amplifier in telecommunications applications are studied theoretically. An axial model is used to predict mechanical, electronic and optical properties of these CQD. A crossover from a dominant TE optical ground state absorption to a TM dominant absorption is predicted for a number of layers equal to about 9 in good agreement with the experiment. The weight of the light hole component of the valence band ground state increases as a function the number of layers. The change of the TE/TM polarization ratio is also associated to a symmetry change of the heavy hole component. A modification of the aspect ratio of the CQD seems to be the most important factor to explain the change of the electronic states configuration as a function of the strain distribution.

P.A.C.S. 71.20.Nr, 73.21.La, 78.20.Hp

[a)]Electronic mail : jacky.even@insa-rennes.fr

Recently, vertically stacked quantum dots (QD) with a very small or zero spacing (columnar QD, CQD) have been investigated in order to obtain polarization insensitive semiconductor amplifiers (SOA) [1]. These experimental results indicate that the TE/TM mode photoluminescence intensity is inverted for a number of QD layers (N) beyond 9 in the InAs/GaAs system. A first theoretical study for InAs/GaAs columnar system up to N=5, shows that the biaxial strain is modified at the center of the CQD by comparison to standard QD [2]. As a consequence, the light hole (LH) component of the hole ground state increases when the number of layer increases or when the QD spacing decreases. This approach has been extended more recently [3] to the InAs/InP system in order to propose SOA operating at 1.55μm. These new SOA will be able to treat random optical signals for general fiber communication. Experimental results have been obtained in our group in the last years concerning the physics and the optimization of devices on similar InAs/InP QD based structures [4-8]. We have also used a complete theoretical description of the electronic properties of such nanostructures [9]. An efficient mechanical and electronic axial approximation of the strained 8x8 Hamiltonian has been proposed for zinc-blende nanostructures with a cylindrical shape on (100) substrates [10-11]. It is possible with this method to treat large systems using conventional finite element computation [12]. We have demonstrated that it is able to describe the complex inhomogeneous strain distribution and electronic properties of InAs/InP QD using cylindrical coordinates $(\boldsymbol{r},\boldsymbol{z})$ [9-11]. In this paper, the strain, electronic and optical properties of InAs/InP CQD are analyzed with this method.

We examine InAs CQD geometries corresponding to the $C_{\infty v}$ symmetry (rotational symmetry around the z-[001]-axis) as shown by the insert of figure 1-a for 7 layers of truncated cones. The chosen dimensions are 1.2 nm for the truncated cone height and 7 nm for the radius. The CQD are embedded into an $In_{0.85}Ga_{0.15}As_{0.33}P_{0.67}$ lattice-matched quaternary

alloy. The authors of ref. [3] have used an $In_{0.66}Ga_{0.34}As_{0.44}P_{0.56}$ tensile strain (1%) quaternary alloy between the layers for strain compensation. The InAs wetting layer usually present during the growth of such Stranski-Krastanow type QD is not specified, so we have decided to use a quaternary alloy with an average composition $In_{0.75}Ga_{0.25}As_{0.58}P_{0.42}$ between the layers. It should be pointed out that the results are almost not affected by the composition of this alloy. The axial 8x8 QD Hamiltonian is block diagonal in a $\boldsymbol{F}_z$ basis, where $\boldsymbol{F}_z = J_z + L_Z$ is the total angular momentum. The basis is constructed in a product form $\left|\boldsymbol{J},\boldsymbol{J}_z\right\rangle\left|\boldsymbol{L}_z = \boldsymbol{F}_z - \boldsymbol{J}_z\right\rangle$ where the first factor corresponds to the band-edge Bloch functions (the (u_1,u_2), (u_4,u_5), (u_3,u_6), (u_7,u_8) bands are respectively related to the conduction band (CB), heavy hole (HH), light hole (LH) and split-off bands (SO)). The variations of the energy of the electronic conduction band (CB) degenerate ground and excited states are represented as a function of the number of layers on figure 1-b. The CB ground state of the CQD corresponds to $\boldsymbol{F}_z = \pm 1/2$ whatever the number of layers like in the case of a single QD [11]. The most striking feature appears for the valence bands (VB) behaviour (figure 1-c). A crossover between $\boldsymbol{F}_z = \pm 3/2$ and $\boldsymbol{F}_z = \pm 1/2$ for the VB ground state is calculated for a number of layers close to 9. We may notice this number corresponds to an aspect ratio of the CQD on the order of 1. A modification of the main confinement effect from vertical to radial is important.

In figure 2, the variations of the HH, LH and CB confinement potentials along the vertical axis are represented for N=9. As it can be seen the values of the HH and LH potentials are similar at the center of the CQD. The biaxial strain component is almost equal to zero in the CQD which is completely different from what is observed in usual flat QD [9-11]. This is also a result of the change in the aspect ratio. The $\boldsymbol{u}_3$ LH (left) and $\boldsymbol{u}_4$ HH (right) components of the (a-b) $\boldsymbol{F}_z = +1/2$ and (c-d) $\boldsymbol{F}_z = +3/2$ VB states are shown on figure 3 for

N=8. In that case (figure 1-c) , the $F_z = +3/2$ state is the VB ground state and the $F_z = +1/2$ is the VB first excited state which is very close in energy. The weights of these two components are indicated above each picture. The weight of the u_4 HH component (79%) is the most important one for the $F_z = +3/2$ VB ground state. In that case, the overlap with the u_2 CB component (94%) of the $F_z = +1/2$ CB ground state is by far the most important one giving rise to a TE polarized absorption. The u_3 LH component of the $F_z = +3/2$ VB ground state is weaker (12%), but the most important feature is that it is almost antisymmetric with respect to a plane symmetry perpendicular to the z axis. The overlap with the symmetric u_2 CB component of the $F_z = +1/2$ CB ground state is therefore almost equal to 0, giving rise to a negligible TM polarized absorption. On the contrary, the u_3 LH component of the $F_z = +1/2$ VB first excited state is symmetric.

The u_3, u_4 components of the (e, f) $F_z = +1/2$ and (g, h) $F_z = +3/2$ VB states are represented on figure 3 in the same order for a number of layers equal to 10 that is beyond the crossover. In that case (figure 1-c) , the $F_z = +1/2$ state is now the VB ground state and the $F_z = +3/2$ is the VB first excited state. It can be observed now (e) that the weight of the u_3 LH component of the $F_z = +1/2$ VB ground state has increased and remains symmetric. The TM polarized absorption of the ground state optical transition is associated to this component. In addition, a TE polarized absorption is predicted at the same energy for the optical transition between the $F_z = +1/2$ CB ground state and the $F_z = -1/2$ VB ground state. It is related to the u_6 LH component of the $F_z = -1/2$ VB ground state which corresponds to the symmetric u_3 LH component of the $F_z = +1/2$ VB ground state (e). We may notice that the u_4 HH component of the $F_z = +3/2$ VB state (h) is now antisymmetric and therefore the TE polarized absorption associated to that state disappears.

We have represented on figure 4, the variation of the TE (straight lines) or TM (dashed lines) polarized absorption spectra for structures with $7 \leq N \leq 12$. The energy of the ground state optical transition decreases when N increases. It is a size effect. For $N<9$, the absorption spectrum is predominantly TE at the ground state optical transition and TM at the first excited state optical transition. For $N>9$, the absorption spectrum at the ground state optical transition is TE and TM with a predominant TM character and the first excited state transition is dark.

We have used an axial model to study the mechanical, electronic and optical properties of CQD. A crossover from a dominant TE optical ground state absorption to a TM dominant absorption is predicted for a number of layers equal to about 9 in good agreement with the experiment. The weight of LH component of the VB ground state increases as a function of the number of layers but the transition of the TE/TM polarization ratio is also associated to a symmetry change of the HH component. The variation of the CQD aspect ratio induces changes in the main confinement effect (from vertical to radial) and in the strain distribution. The electronic states configuration is strongly affected, particularly in the valence band.

References

[1] T. Kita, P. Jayavel, O. Wada, H. Ebe, Y. Nakata and M. Sugawara, Phys. Stat. Sol. (c) **4** 1137 (2003)

[2] T. Saito, T. Nakaoka, T.Kakitsuka, Y. Yoshikuni and Y. Arakawa, Physica E **26** 217 (2005).

[3] K. Kawagushi, M. Ekawa, N. Yasuaka, T/ Akiyama, H. Ebe, M. Sugawara and Y. Arakawa, Phys. Stat. Sol. (c) **3** 3646 (2006)

[4] C. Cornet, C. Levallois, P. Caroff, H. Folliot, C. Labbe, J. Even, A. Le Corre et S. Loualiche, Appl. Phys. Lett. **87** 233111 (2005)

[5] C. Cornet, C. Labbe, H. Folliot, J. Even, P. Caroff, C. Levallois, O. Dehaese, N. Bertru, A. Le Corre et S. Loualiche, Appl. Phys. Lett. **88** 171502 (2006)

[6] C. Cornet, M. Hayne, P. Caroff, C. Levallois, L. Joulaud, E. Homeyer, C. Paranthoen, J. Even, C. Labbe, H. Folliot, V. V. Moshchalkov and S. Loualiche, Phys. Rev. B **74** 245315 (2006).

[7] E. Homeyer, R. Piron, F. Grillot, O. Dehaese, K. Tavernier, E. Macé, J. Even, A. Le Corre et S. Loualiche, Jap. J. Appl. Phys. **46** 6903 (2007)

[8] K. Veselinov, F. Grillot, C. Cornet, J. Even, A. Bekiarski, M. Gioannini et S. Loualiche, IEEE J.Quant. Elec. **43** 810 (2007)

[9] C. Cornet, A. Schliwa, J. Even, F. Dore, C. Celebi, A. Letoublon, E. Mace, C. Paranthoen, A. Simon, P. M. Koenraad, N. Bertru, D. Bimberg and S. Loualiche, Phys. Rev. **B74** 035312 (2006)

[10] J. Even, F. Doré, C. Cornet, L. Pédesseau, A. Schliwa and D. Bimberg, Appl. Phys. Lett. **91** 122112 (2007).

[11] J. Even, F. Doré, C. Cornet and L. Pédesseau, Phys. Rev. **B77** 085305 (2008).

[12] Femlab 3.2 software, Trademark of Comsol AB (2005).

Figure captions

Figure 1: As an example, we show InAs CQD geometry corresponding to N=7 layers of truncated cones (a). Dependence of the electronic Conduction Bands ($F_z = \pm 1/2$ straight lines and $F_z = \pm 3/2, \pm 5/2, \pm 7/2$, dashed lines) (b) and of the electronic Valence Bands ($F_z = \pm 1/2$ straight lines and $F_z = \pm 3/2, \pm 5/2$, dashed lines) (c) versus the number of layers.

Figure 2: Evolution of the CB, HH (straight lines), LH (dashed line) confinement potentials represented for N=9.

Figure 3: The u_3 LH (a, c) and u_4 HH (b, d) components of the $F_z = +1/2$ and $F_z = +3/2$ VB states are shown for N=8. Idem for N=10 with u_3 LH (e, g) and u_4 HH (f, h) components of the $F_z = +1/2$ and $F_z = +3/2$ VB states.

Figure 4: Dependence of the TE (straight line) and TM (dashed line) polarized absorption spectra for structures within the interval 7≤N≤12.

FIG. 1.

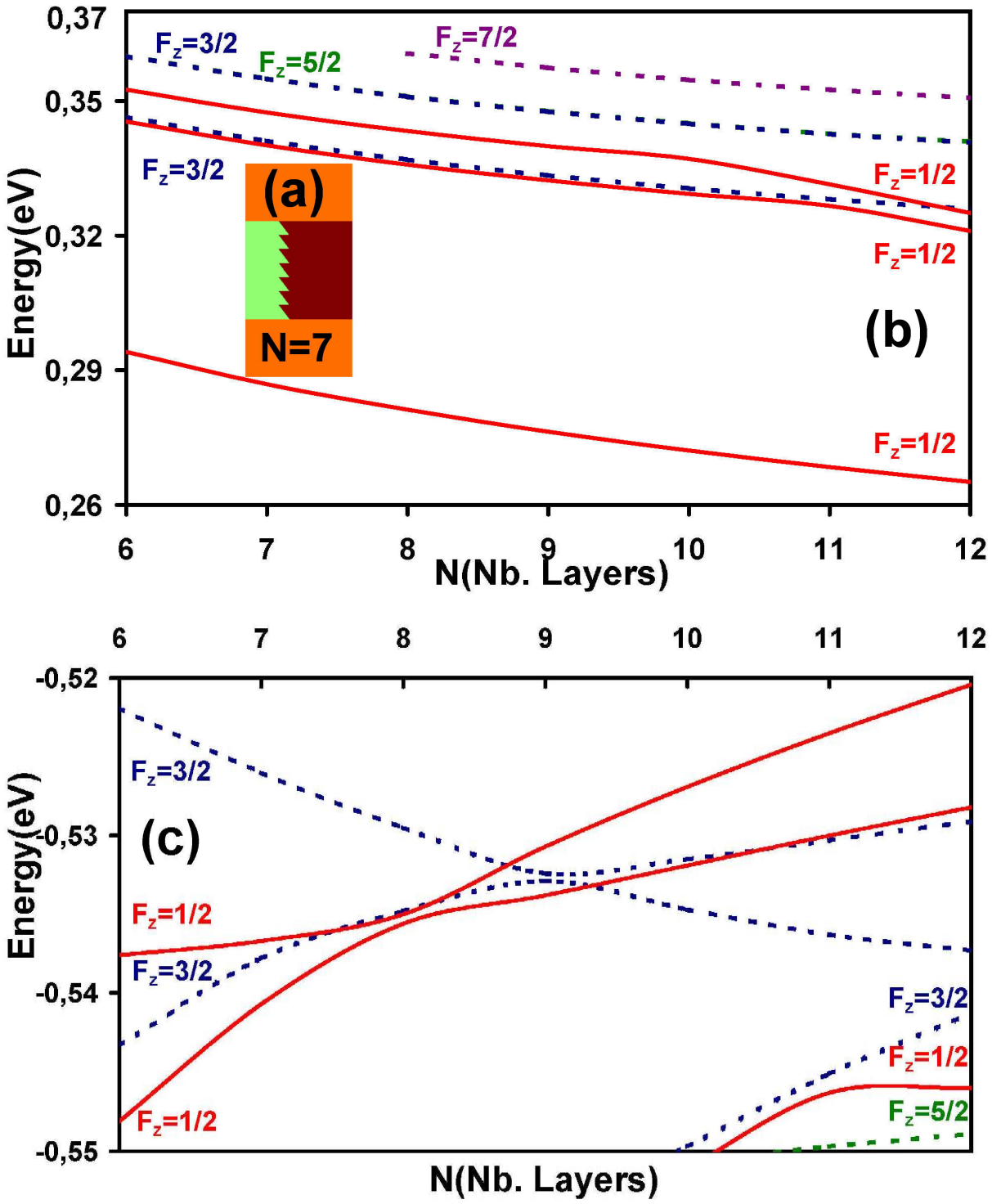
0,37
0,35
0,32
0,29
0,26
Energy(eV)
F_z=3/2
F_z=5/2
F_z=7/2
F_z=3/2
(a)
N=7
F_z=1/2
F_z=1/2
(b)
F_z=1/2
6
7
8
9
10
11
12
N(Nb. Layers)
-0,52
-0,53
-0,54
-0,55
Energy(eV)
F_z=3/2
(c)
F_z=1/2
F_z=3/2
F_z=3/2
F_z=1/2
F_z=1/2
F_z=5/2
N(Nb. Layers)

FIG. 2

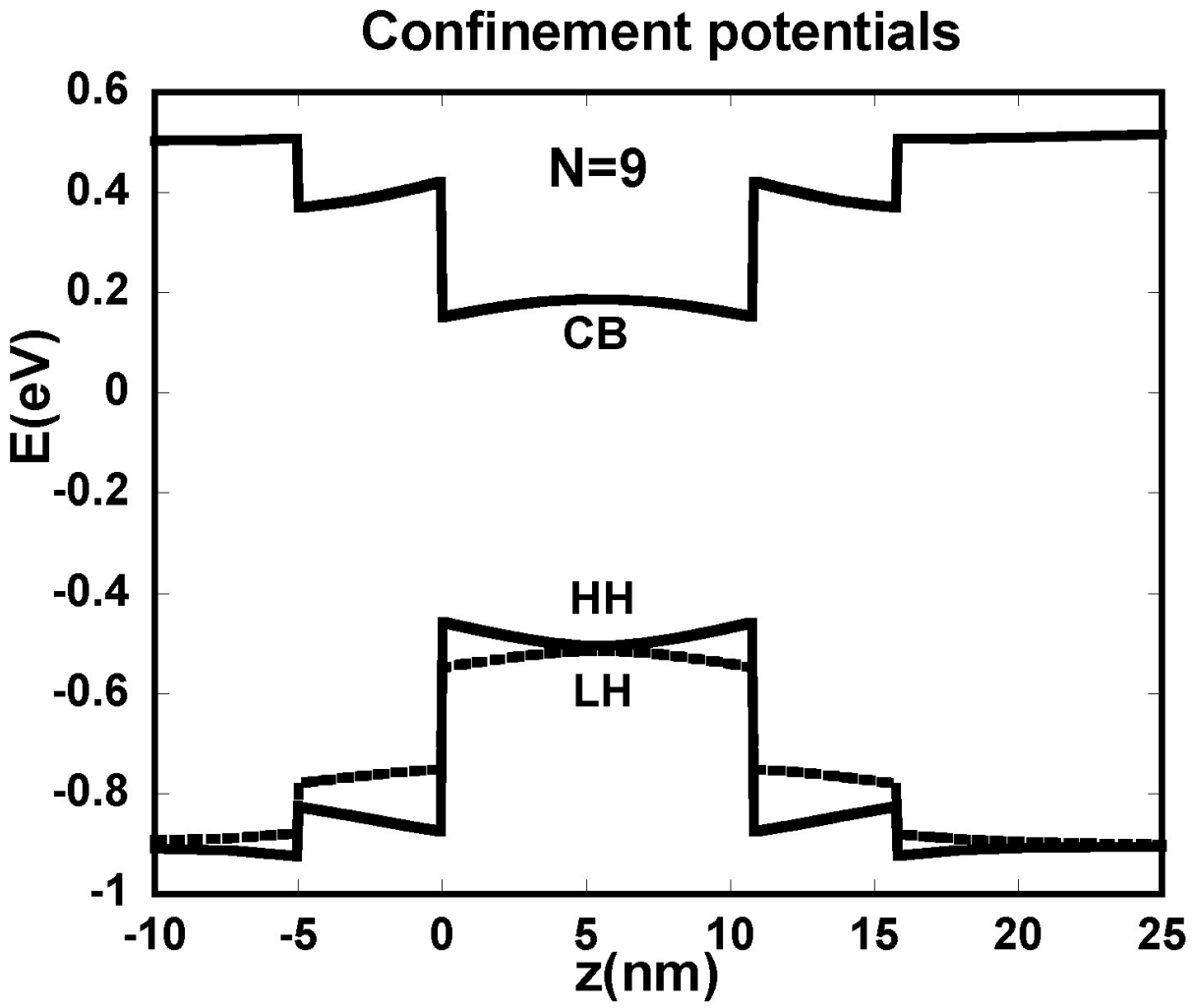
Confinement potentials
N=9
CB
HH
LH
E(eV)
z(nm)
0.6
0.4
0.2
0
-0.2
-0.4
-0.6
-0.8
-1
-10
-5
0
5
10
15
20
25

FIG.3

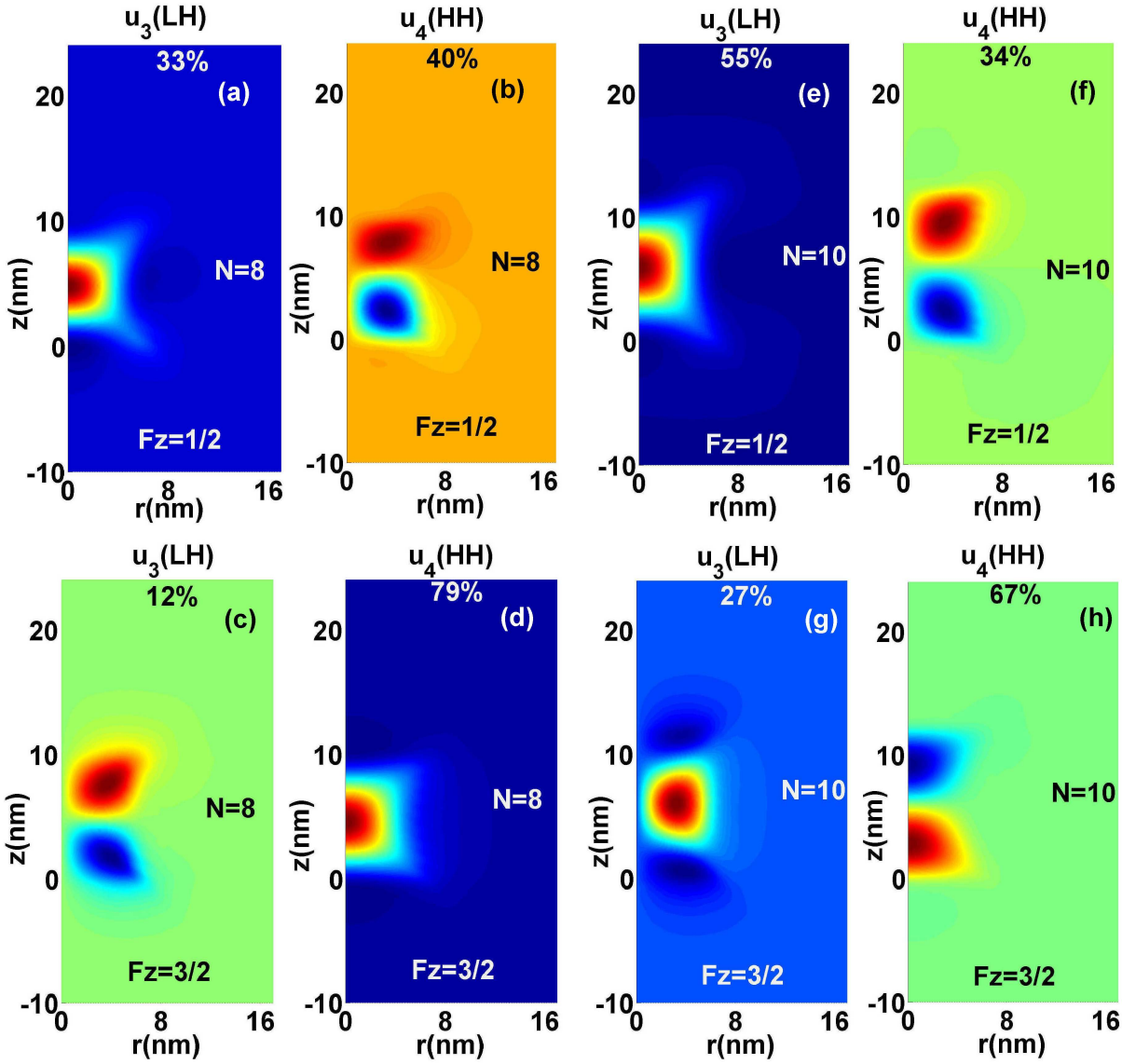
u3(LH)
33%
(a)
N=8
Fz=1/2
u4(HH)
40%
(b)
N=8
Fz=1/2
u3(LH)
55%
(e)
N=10
Fz=1/2
u4(HH)
34%
(f)
N=10
Fz=1/2
u3(LH)
12%
(c)
N=8
Fz=3/2
u4(HH)
79%
(d)
N=8
Fz=3/2
u3(LH)
27%
(g)
N=10
Fz=3/2
u4(HH)
67%
(h)
N=10
Fz=3/2
z(nm)
r(nm)
20
10
0
-10
0
8
16

FIG. 4.

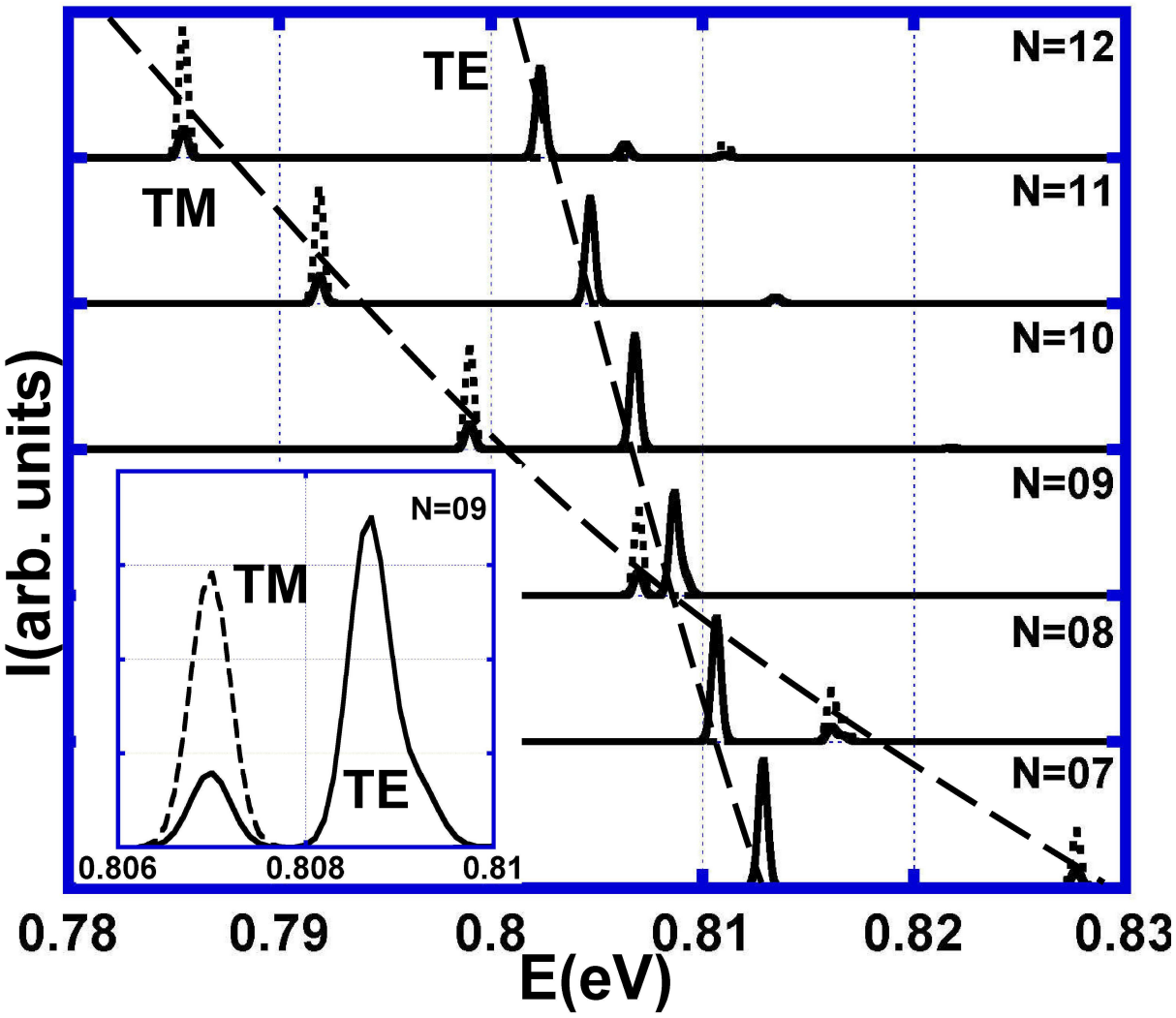
TE
TM
N=12
N=11
N=10
N=09
N=08
N=07
N=09
TM
TE
0.806
0.808
0.81
I(arb. units)
0.78
0.79
0.8
0.81
0.82
0.83
E(eV)